Particle Accelerators, 1997, Vol. 57, pp. 159–173
Reprints available directly from the publisher
Photocopying permitted by license only

LONGITUDINAL BEAM TRANSFER FUNCTION DIAGNOSTICS IN AN ELECTRON STORAGE RING

JOHN BYRD

Lawrence Berkeley National Laboratory, 1 Cyclotron Road, Berkeley, CA 94720, USA

(Received 8 April 1997; Revised 30 May 1997; In final form 3 June 1997)

We describe the technique of longitudinal beam transfer function (BTF) for measuring several properties of longitudinal oscillations in an electron storage ring such as the synchrotron frequency, radiation damping time, and bunch length. We show how the BTF for center-of-charge oscillations is related to the distribution of synchrotron frequencies within the bunch and present the analytic solution of the BTF for a Gaussian distribution of longitudinal oscillation amplitudes within the bunch at very low current and the dependence of synchrotron frequency on amplitude. We compare the results with measurements made at the Cornell Electron Storage Ring (CESR) and the Advanced Light Source (ALS).

Keywords: Beam diagnostics; Electron storage ring; Synchrotron oscillations

I. INTRODUCTION

Beam transfer function (BTF) diagnostics are used in almost all storage rings for measuring the betatron and synchrotron frequencies. In the simplest case, a swept frequency drive excites either betatron or synchrotron oscillations while a beam signal is observed on a spectrum analyzer. In other applications, BTF techniques have been used[1–3] for measuring beam impedance and feedback loop stability. The BTF is also used extensively as an example in descriptions of the phenomenon of Landau damping.[4,5] We describe in this paper an application of the BTF technique for use in an electron storage ring for making measurements of the distribution of synchrotron frequencies within

a single bunch at low beam current. By taking advantage of the Gaussian distribution in the energy spread within the bunch resulting from the quantum nature of the emission of synchrotron radiation and the sinusoidal RF voltage, we can use the measurements to derive a relatively precise measure of the nominal synchrotron frequency, the longitudinal radiation damping rate, and the bunch length. Although these parameters can be measured using other techniques, the BTF method has the advantage of being relatively simple and inexpensive, and typically uses equipment that is either already available in the control room or easily assembled. The BTF technique can potentially be used to study the effects of short range wakefields and the longitudinal beam dynamics of more complicated situations such as double RF systems and low momentum compaction.

In general, the BTF is defined as the ratio of the beam response to an external excitation as a function of frequency. Over all frequencies, the BTF is simply the Fourier transform of the impulse response of the beam. In practice, either a vector or scalar network or FFT analyzer is used to supply a swept frequency or noise excitation to the beam via either a stripline kicker or RF cavity and the beam response is measured through a pickup. For the cases discussed in this paper, we excite longitudinal oscillations by phase modulating the voltage in the fundamental mode of an RF cavity and measure the synchrotron oscillations by detecting the phase of a beam pickup signal relative to a fixed reference phase or by measuring energy oscillations at a point of dispersion in the lattice. It is also assumed throughout the paper that the amplitude of synchrotron oscillations is small enough that the motion can be described as linear.

Section 2 discusses the longitudinal beam distribution and gives a physical interpretation of the transfer function for a Gaussian distribution. Section 3 presents the measurements performed at the Advanced Light Source (ALS) and the Cornell Electron Storage Ring (CESR). The Vlasov approach to calculation of the BTF is given in the appendix.

II. BEAM TRANSFER FUNCTION FOR A GAUSSIAN DISTRIBUTION

The energy distribution in an electron bunch in a storage ring is Gaussian, resulting from the balance of the quantum excitation from

synchrotron radiation emission and radiation damping.[8] It can be shown that the phase space density distribution to second order is given by

$$\psi_0(\hat{\tau}) = \frac{1}{2\pi\sigma_\tau^2} e^{-(\hat{\tau}^2/2\sigma_\tau^2)}, \tag{1}$$

where $\hat{\tau}$ is the oscillation amplitude and σ_τ is the RMS bunch length, both in units of time. The nonlinearity of the sinusoidal RF voltage results in a synchrotron frequency dependent on the amplitude of phase oscillation of the form

$$\omega_s(\hat{\tau}) = \omega_{s0}(1 - \mu\hat{\tau}^2), \tag{2}$$

where

$$\mu = \frac{\omega_{RF}^2\left(1 + \frac{5}{3}\tan^2\phi_s\right)}{16} \approx \frac{\omega_{RF}^2}{16}, \tag{3}$$

where ϕ_s is the synchronous phase angle. For most cases, the effect of ϕ_s can be ignored.

The combination of the distribution of oscillation amplitudes and synchrotron frequency as a function of amplitude yields a unique distribution of synchrotron frequencies within the bunch for a given bunch length. As described below, the natural spread in frequencies leads to Landau damping of coherent oscillations. We can estimate the spread as the difference in synchrotron frequency of an electron oscillating with infinitesimal amplitude compared with an electron oscillating with 2.5 times the RMS amplitude, given approximately by

$$\Delta\omega_s \approx 0.4\alpha\sigma_\varepsilon\omega_{RF}^2\sigma_\tau, \tag{4}$$

where σ_ε is the RMS fractional energy spread, α is the momentum compaction, and ω_{RF} is the angular RF frequency. For example, plotted in Figure 1 is the frequency spread in the bunch as a function of the RMS bunch length for both ALS and CESR parameters. A constant energy spread is assumed. The spread in frequencies is roughly equivalent to the damping rate of center-of-charge oscillations

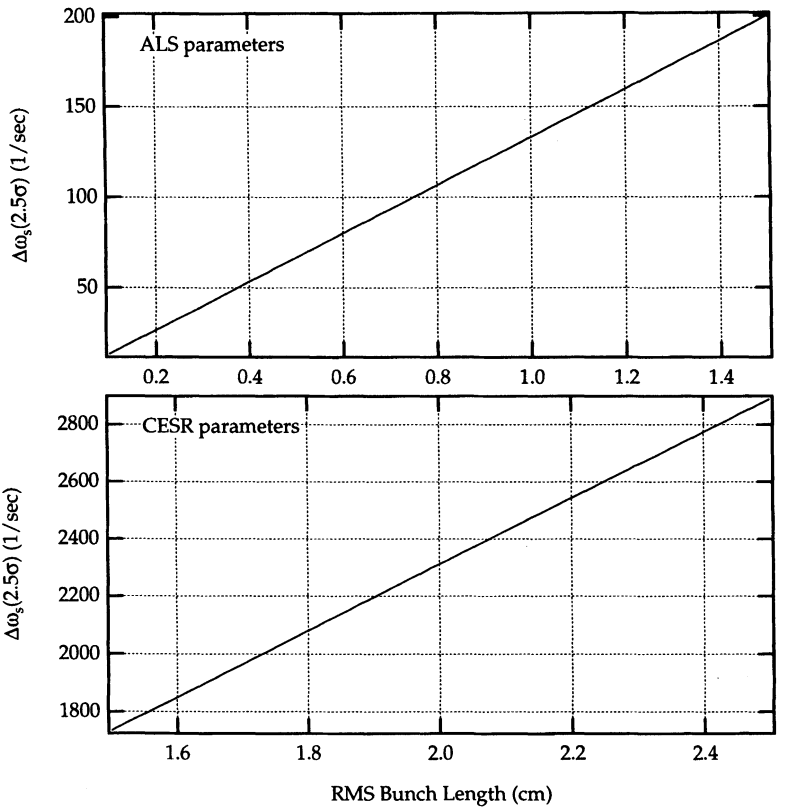

FIGURE 1 Estimated incoherent synchrotron frequency spread for ALS and CESR parameters. The radiation damping rate for both cases is about 75/s.

from decoherence. It is useful to compare this with the synchrotron radiation damping rate which, coincidentally, for both cases is about 75/s. For the case of the ALS, the synchrotron radiation damping is comparable with the decoherence rate but for the CESR case the radiation damping rate is negligible. The significance of this on the BTF is discussed further below.

Given the distribution, the BTF can be found by solving the Vlasov equation for a small perturbation of the phase space distribution at the excitation frequency and integrating to find the first moment of the distribution. This approach is identical to that used in finding the stability conditions of coherent instabilities. It is described in more

detail in the appendix. Equivalently, the BTF can be found by calculating moments of the distribution in response to an impulse excitation in the time domain and making a Fourier transform on the result. The time domain impulse response has been calculated[9] and can be shown to give the same result as the Vlasov approach for infinitesimal excitation. As shown in the appendix, the BTF can be expressed in terms of a dispersion integral given by

$$I(\omega_m) \propto \int_0^\infty \frac{\hat{\tau}^2 \, d\hat{\tau}}{\omega_m - \omega_s(\hat{\tau})} \frac{\partial \psi_0}{\partial \hat{\tau}}, \tag{5}$$

where ω_m is the angular modulation frequency. Radiation damping is included by making the synchrotron frequency complex as given by

$$\tilde{\omega}_s = \omega_s + j\lambda_{rad}. \tag{6}$$

For a Gaussian distribution in oscillation amplitude, the dispersion can be expressed in terms of the exponential integral.[10]

Consider first the case of no radiation damping ($\lambda_{rad} = 0$). The amplitude and phase of the BTF is plotted for several values of the bunch length in Figure 2. For convenience, we have used the convention that the phase goes from 180° to 0° passing from far below the nominal synchrotron frequency to above. In practice, the absolute phase is determined by other phase shifts in the system such as cable delays, etc. A physical interpretation of Eq. (5) yields some insight into the behavior of the transfer function. When the external excitation frequency is greater than the zero-amplitude synchrotron frequency, the phase of the beam response does not vary with frequency because all of the electrons within the bunch are being driven above their resonant frequency. When $\omega_m < \omega_{s0}$ and the external excitation frequency is within the spread of incoherent frequencies, some of the particles in the bunch are being driven resonantly, some below resonance, and some above resonance and thus there is a net phase shift between the drive and the response. When the external excitation frequency is far below the synchrotron frequency, all electrons have again the same phase response. Neither the amplitude and phase response are symmetric in frequency because the distribution of synchrotron frequencies with oscillation amplitude is not symmetric. Note

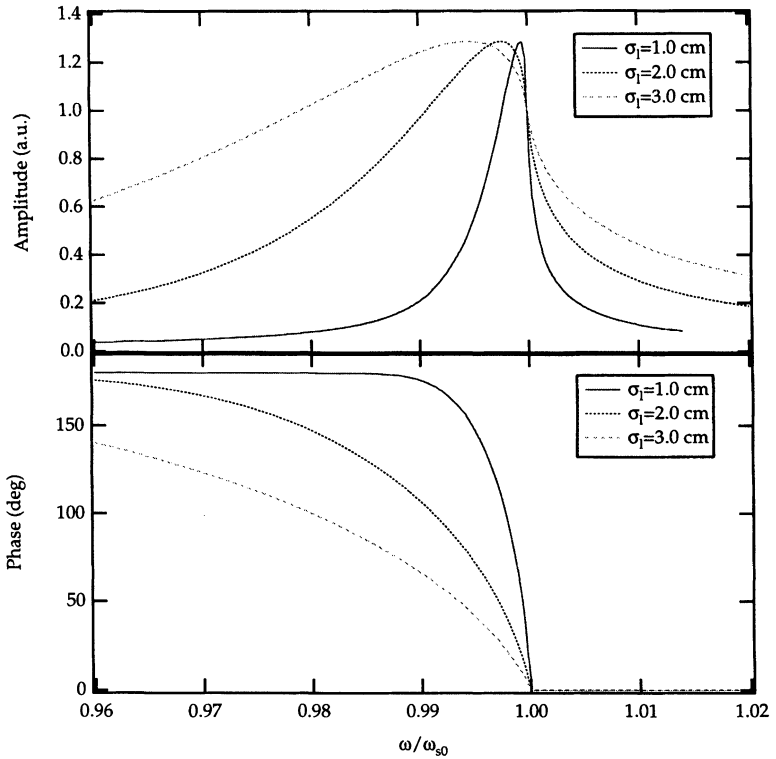

FIGURE 2 Calculated BTF for as a function of bunch length for the case of no radiation damping.

that the cusp in the phase response corresponds to the nominal synchrotron frequency and that the peak amplitude response does not occur at this frequency but slightly below.

We can also interpret the BTF mathematically. As the excitation frequency decreases, a phase shift enters when $\omega_m < \omega_{s0}$ because there is now a pole at the amplitude $\hat{\tau}$ where the denominator vanishes. The imaginary part of the dispersion integral in this region also accounts for the Landau damping of the oscillations.[6,7]

Figure 3 shows a plot of the BTF for the case of nonzero radiation damping. The physical interpretation of the response is the same as above except that the response of individual electrons now have a natural width due to the radiation damping. This tends to smear the response of the distribution of synchrotron frequencies. As the width

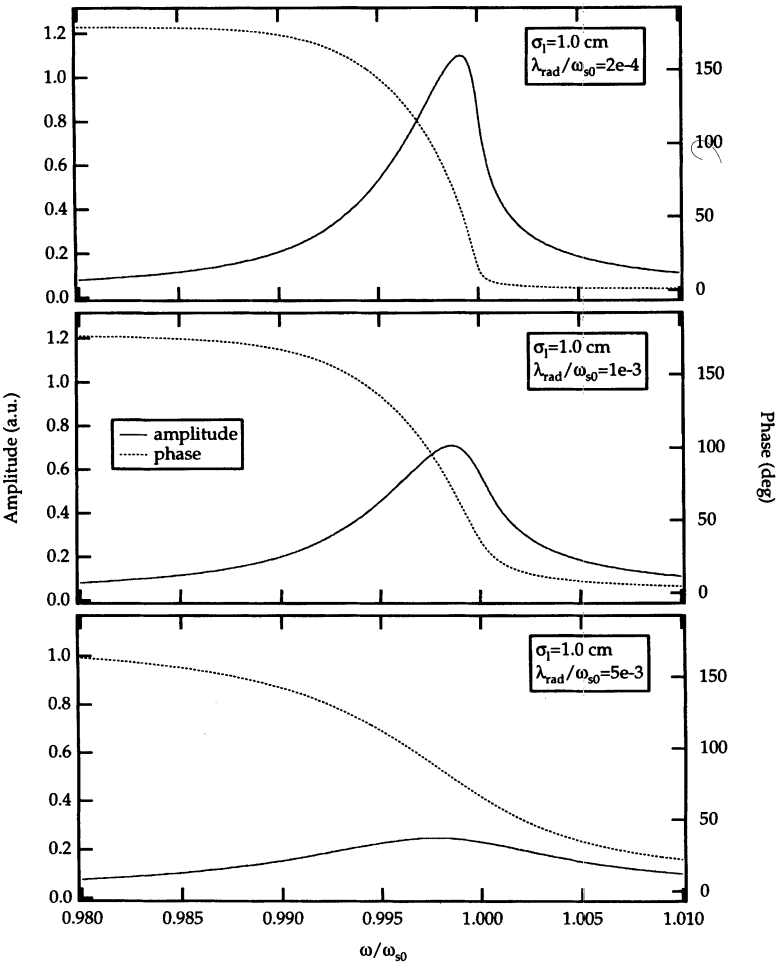

FIGURE 3 Calculated BTF for a 1 cm RMS bunch length as a function of increasing radiation damping, which is expressed relative to the synchrotron frequency.

due to radiation damping approaches the width of the distribution of synchrotron frequencies, the response becomes much more like the Lorentzian shape expected from a damped harmonic oscillator. As the spread in frequencies within the bunch decreases relative to the radiation damping rate, the bunch behaves more like a single damped harmonic oscillator. Note also that the dispersion integral no longer has a pole.

III. BEAM MEASUREMENTS

The setup for measurement of the BTF for the ALS and CESR measurements is shown in Figure 4. Relevant parameters of both rings are given in Table I. In both cases, we excited longitudinal oscillations by phase modulating (PM) the RF voltage. This was achieved by injecting the modulation signal as an error signal in the RF phase control feedback loop.[11]

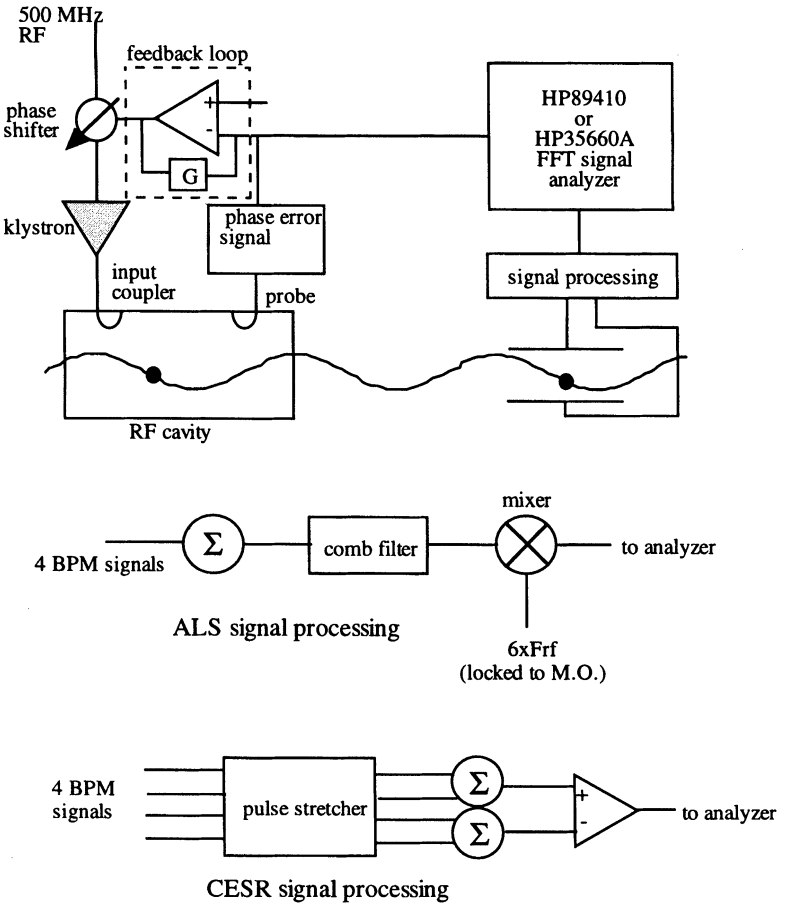

FIGURE 4 General setup for longitudinal BTF measurements. The signal processing techniques used at ALS and CESR are shown separately.

TABLE I ALS and CESR parameters used in measurements

Symbol	*Description*	*ALS*	*CESR*
E	Beam energy (GeV)	1.5	5.2
C	Circumference (m)	196.8	768.4
f_{RF}	RF Frequency (MHz)	500	500
α	Mom. compaction	1.59e−3	1.54e−2
Q_s	Synchrotron tune	0.0038–0.0075	0.05
λ_{rad}	Long. rad damping rate (1/turn)	4.9e−5	3.7e−4

For the ALS measurements, synchrotron oscillations were detected using the phase detector for an existing longitudinal coupled-bunch feedback system.[12] This detector passes the sum of the signal from four capacitive button BPMs (beam position monitors) located at one point in the ring through a 4-tap comb filter with a center frequency of 3 GHz ($6 \times \omega_{RF}/2\pi$). To first order, the sum of the four button signals is not sensitive to the transverse position of the beam. The signal is demodulated to baseband through a double balanced mixer using a 3 GHz local oscillator derived from the 500 MHz master oscillator. Detection at the sixth RF harmonic increases the sensitivity to phase oscillations compared to detection at the RF frequency and is also near the frequency of maximum pickup impedance of the BPMs. Because of the relatively short bunch length in the ALS, the 3 GHz component of the beam signal is reduced very little compared to the 500 MHz component. For CESR measurements, synchrotron oscillations were detected by measuring energy oscillations as horizontal displacement at a point of high dispersion in the lattice. The horizontal displacement was found from the difference of button BPMs. Any betatron motion could be ignored because the betatron frequency is far from the synchrotron frequency.

The sensitivity required for the detection of the synchrotron oscillations depends somewhat on the storage ring parameters. For example, to obtain the most accurate results, we found that it was important to excite the synchrotron oscillations with an amplitude at significantly less than the natural bunch length in order that the oscillations remained quasi-linear. We empirically determined the optimum level of excitation by lowering the excitation level until the shape of the transfer function remained constant. Thus, measurements with shorter bunch length require greater sensitivity. We independently

verified the amplitude of PM in the cavity by measuring the spectrum of PM sidebands present on a cavity probe signal with no beam. The ratio of first order sidebands to the carrier frequency is given by the ratio of $J_1(\phi)/J_0(\phi)$, where $J_n(\phi)$ is the nth order Bessel function and ϕ is the amplitude of PM. Also, to avoid conversion of PM to amplitude modulation, the frequency of the RF cavity was tuned to on resonance with the RF drive frequency for all measurements. For the conditions of these measurements, the variation of the cavity response over the bandwidth of the measurement was negligible.

An FFT signal analyzer was used as the source and receiver for the signal for both measurements. We found that for a given level of excitation, a better signal/noise ratio could be achieved using a bandwidth limited noise source than for a swept frequency excitation. In principle both approaches yield the same results.

In order to avoid the influence of collective effects on the bunch shape, all of the measurements presented here were made at the lowest single bunch current possible which still gave a reasonable signal level. For both the ALS and CESR measurements, we used a bunch current of 100–300 μA, well below the threshold for any instabilities and low enough that potential well distortion is negligible.

Shown in Figures 5 and 6 are BTFs measured at CESR and ALS, respectively, for various beam energies and synchrotron frequencies. Each result is fitted to the functional form given in Eq. (16). For the CESR measurements, the BTF is dominated by the effect of the spread in synchrotron frequencies. However, the effect of radiation damping, although relatively small, is still evident near the zero-amplitude synchrotron frequency. A fit to the data assuming no radiation damping is also shown in one of the measurements for comparison. Unfortunately, no other independent means to accurately measure the bunch length were available. To compare the fit values with the expected values, we used the predicted energy spread and momentum compaction along with the fit value of the zero-amplitude synchrotron frequency to determine the bunch length. This value is shown in parentheses next to the fit value and is in very good agreement with the measured value. The fit value for the radiation damping also agrees well with the expected value for a beam energy of 5.2 GeV although the fit is not very sensitive for these conditions.

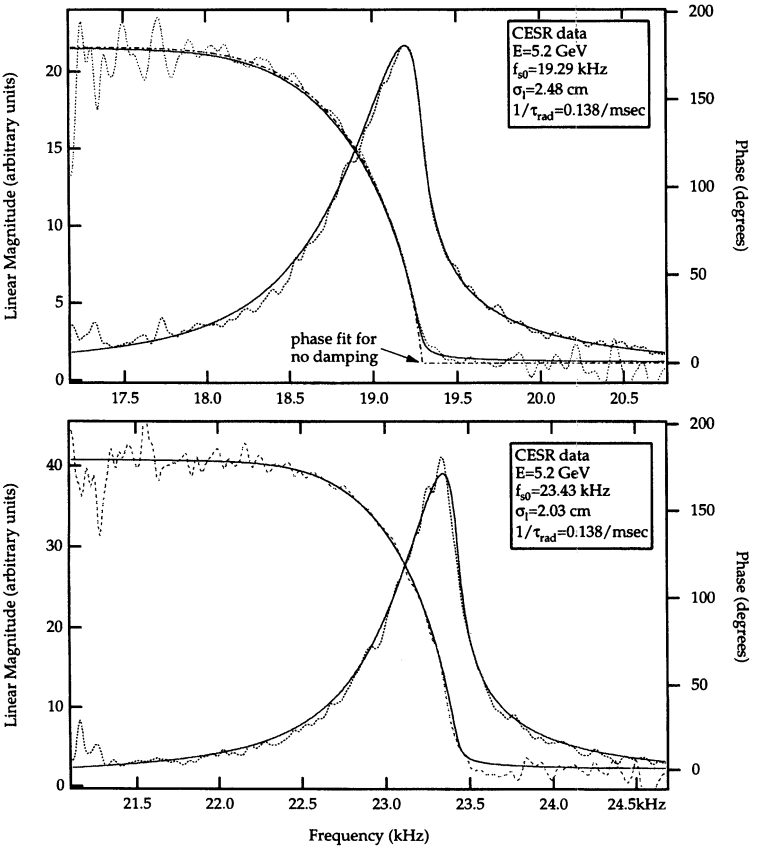

FIGURE 5 Results of BTF measurements at CESR for two nominal bunch lengths.

For the ALS measurements, the width of the amplitude response is due in roughly equal parts to the radiation damping and the spread of synchrotron frequencies and thus the BTF is much more symmetric. We independently measured the bunch length with a streak camera. Measured values from a streak camera are shown for comparison (in parentheses). Although the agreement for the values of the bunch length is good, it is less precise for the case when the decoherence rate and the radiation damping rate are comparable. If the interest is in measuring bunch length, the BTF technique would be limited to relatively long bunches.

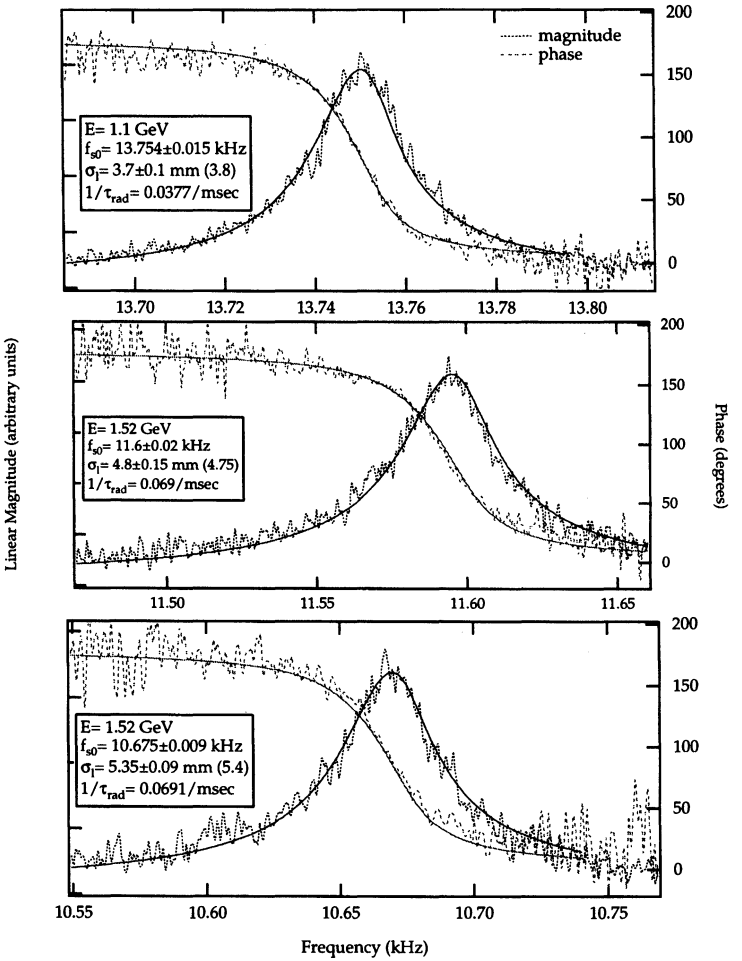

FIGURE 6 Results of BTF measurements at ALS for several energies and nominal bunch lengths.

IV. CONCLUSIONS

The BTF is a relatively simple method for measuring the incoherent spread in synchrotron frequencies in a single bunch. With a careful analysis, the small amplitude synchrotron frequency, the longitudinal radiation damping rate, and the bunch length can all be inferred from this measurement. The precision of the measurement depends primarily

on the value of the radiation damping rate compared with the spread in synchrotron frequencies. The measurement of the bunch length is more precise when $\lambda_{\text{rad}} < \Delta\omega_s$ and vice versa for measurement of the radiation damping time.

We are hopeful that this technique can be used for measuring the effects of distortions of the phase space distribution due to instabilities or other effects. We are grateful for discussions with Albert Hofmann and Flemming Pedersen and for assistance from Miguel Furman in interpreting the complex integrations in Eq. (15). We would like to thank the operations groups of ALS and CESR for assistance with the measurements. We also thank the National Science Foundation for support of the CESR measurements.

References

[1] D. Mohl and A.M. Sessler, *Proc. 8th Int. Conf. High Energy Accel.*, p. 334.
[2] A. Hofmann and B. Zotter, *Proc. 1977 IEEE Part. Accel. Conf.*, p. 1487.
[3] J.M. Jowett *et al.*, *Proc. 1987 IEEE Part. Accel. Conf.*, p. 726.
[4] A. Hofmann, *Proc. of 1989 CERN Acc. School*, CERN 89-01, p. 40.
[5] J. Gareyte, *Proc. of 1987–88 US Acc. School*, AIP 184, p. 343.
[6] H.G. Hereward, CERN 65-20 (1965).
[7] H.G. Hereward, CERN 69-11 (1969).
[8] M. Sands, SLAC-121 (1970).
[9] H. Moshammer, *NIMA* **323**, 553 (1992).
[10] M. Abromowitz and I.A. Stegun, *Handbook of Mathematical Functions*, Dover (1965), p. 228.
[11] C.C. Lo, B. Taylor and K. Baptiste, *Proc. 1995 IEEE Part. Accel. Conf.*, p. 801.
[12] J.D. Fox *et al.*, *Proc. 1996 European Part. Accel. Conf.*

APPENDIX: VLASOV SOLUTION FOR THE BEAM TRANSFER FUNCTION

In the presence of the external driving force, the second order equation for τ is

$$\ddot{\tau} + 2\lambda_{\text{rad}}\dot{\tau} + \omega_s^2\tau = g_0 e^{j\omega_m t}, \tag{7}$$

where τ is the time displacement of the electron from the synchronous electron, λ is the radiation damping rate, g_0 is the amplitude of the driving force and is assumed to be small.

Consider an external longitudinal excitation applied to a single bunch which creates a small dipole perturbation to the phase space density. For a small excitation, the phase space density has the form

$$\psi(\hat{\tau}, \theta; t) = \psi_0(\hat{\tau}) + \psi_1(\hat{\tau}) e^{j(\omega_m t - \theta)}, \tag{8}$$

where ω_m is the angular frequency of the phase modulation, θ is the azimuthal angle in phase space, ψ_0 is the unperturbed phase space density and ψ_1 is a small perturbation. The perturbation revolves in phase space at frequency ω. It is assumed that $\psi_1 \ll \psi_0$.

To find the BTF for centroid oscillations, we must find the first moment of the distribution given in Eq. (8). However, first we must solve for the perturbation ψ_1 which can be done by applying the Vlasov equation. Although there are phase space density fluctuations for electron beams, the phase space is conserved on average. Radiation damping is included by taking the synchrotron oscillation frequency as complex given by

$$\tilde{\omega}_s = \omega_s - j\lambda_{rad}. \tag{9}$$

The Vlasov equation can be written as

$$\frac{d\psi}{dt} = \frac{\partial \psi}{\partial t} + \frac{\partial \psi}{\partial \hat{\tau}} \frac{\partial \hat{\tau}}{\partial t} + \frac{\partial \psi}{\partial \theta} \frac{\partial \theta}{\partial t} = 0, \tag{10}$$

where the spatial derivatives are taken with respect to the polar coordinates $\hat{\tau}$ and θ.

Combining Eqs. (7) and (10), the phase space perturbation can be found to be

$$\psi_1(\hat{\tau}) = \frac{g_0}{2\omega_s(\omega - \omega_s)} \frac{\partial \psi_0}{\partial \hat{\tau}}. \tag{11}$$

The center-of-charge motion is found as the first moment of the perturbed distribution and is given by

$$\bar{\tau}(t) = \frac{g_0}{2} \int_0^{2\pi} d\theta \int_0^{\infty} \hat{\tau}\, d\hat{\tau} \frac{\hat{\tau} \cos\theta}{\omega_s(\omega - \omega_s)} \frac{\partial \psi_0}{\partial \hat{\tau}} e^{j(\omega t - \theta)}. \tag{12}$$

Again, for $\omega \approx \omega_s$, the denominator in the integral can be rewritten such that the centroid motion is

$$\bar{\tau}(t) = \frac{g_0}{\omega} I(\omega) e^{j\omega t}, \tag{13}$$

where $I(\omega)$ is known as the dispersion integral and is given by

$$I(\omega) \equiv \frac{\pi}{2} \int_0^\infty \frac{\hat{\tau}^2 \, d\hat{\tau}}{\omega_m - \omega_s(\hat{\tau})} \frac{\partial \psi_0}{\partial \hat{\tau}}. \tag{14}$$

It is interesting to note that the Vlasov solution for the centroid motion contains an integration over the derivative of the phase space density rather than the phase space density itself. The reason for this[6,7] is that the observed signal is the deviation of the distribution from the nominal distribution and not the distribution itself.

For a Gaussian equilibrium phase space density given in Eq. (1) and an amplitude-dependent synchrotron frequency of the form given in Eq. (2), the dispersion integral can be solved analytically. Substituting

$$\eta = \frac{\hat{\tau}^2}{2\sigma_\tau^2} \quad \text{and} \quad x = \frac{8(\omega_{s0} - \omega - j\lambda_{rad})}{\omega_{s0}\omega_{RF}^2 \sigma_\tau^2},$$

the dispersion integral is given as

$$I(x) \propto \int_0^\infty \frac{\eta e^{-\eta}}{\eta - x} d\eta, \tag{15}$$

$$I(x) \propto 1 - xE_1(x)e^{-x}. \tag{16}$$

For the case when x is real, there is a pole along the real axis when $\eta = x$. In this case the solution can be written as

$$I(x) = \begin{cases} 1 - xe^{-x} \operatorname{Ei}(x) + j\pi x e^{-x} & \text{for } x \geq 0, \\ 1 - |x| e^{-|x|} \operatorname{Ei}(|x|) & \text{for } x < 0. \end{cases} \tag{17}$$